Audio Engineering Society

Convention Paper

Presented at the 146th Convention
2019 March 20–23, Dublin, Ireland

Optimized Exciter Positioning Based on Radiated Sound Power of a Flat Panel Loudspeaker

Benjamin, Zenker[1], Shanavaz S., Abdul Rawoof[1], Sebastian, Merchel[1] and M. Ercan, Altionsoy[1]

[1] *Chair of Acoustics and Haptic Engineering, Dresden University of Technology, 01062 Dresden, Germany.*

Correspondence should be addressed to Benjamin Zenker (benjamin.zenker@tu-dresden.de)

ABSTRACT

Loudspeaker panels, such as distributed mode loudspeakers (DML), are a promising alternative approach in loudspeaker design. DML have many advantages compared to pistonic loudspeakers. However, the frequency response is mostly associated with higher deviations. The position of the excitation is one parameter to optimize the frequency response. An electro-mechanical-acoustical model is presented that enables the optimization of the exciter location, based on the response of the radiated sound power. A simulation model is presented for different surface areas and aspect ratios of the panel. The appropriated positioning and its excitation are discussed based on a single criterion and finally compared with the State of the Art method.

1 Introduction

Distributed mode loudspeakers (DML) are a promising alternative approach in loudspeaker design. The sound is generated by the excitation of plate bending waves, which travel across the surface of the panel. The radiated sound is diffuse in nature. Numerical simulation methods, such as finite element analysis (FEA) and the boundary element method (BEM), can be used to analyze the complex acoustic field, which is generated by panel loudspeakers. Several studies [1–3] showed that simulations tools are needed to improve the acoustic quality of DML.

The radiated sound power response of a DML is typically not flat, and equalization of the input signal is required [4, 5]. The frequency response of a DML is associated with higher deviation compared to loudspeakers with piston behavior. Especially at low frequencies, where the number of modes is small. The positioning of the excitation is one parameter to optimize the frequency response. For an infinite panel, the location of the drive point is meaningless, but not so for a finite panel. There are various approaches to place an exciter on the panel.

Bank describes an approach, where the exciter is positioned at a point that couples to all panel modes [6]. Generally, the exciter should not be placed at a nodal line, where modal displacements are at a minimum. Bank recommended overlaying the first 20 sets of modes to find suitable candidates as drive points. Anderson focused on structures driven by an array of exciters. Individual filtering of every exciter results in a more even response across the defined frequency band [7].

Because the radiation pattern of DML panels strongly depends on frequency, it is not possible to characterize the acoustic behavior of a DML with a small number of measurement points [8]. Azima describes the power response as the acoustic criterion that correlates best with subjective performance [2].

This paper employs optimization of the overall radiated sound power as fitness criterion for the subjective acoustic performance. The linearity of the power transfer function is calculated with a single value. This quality index is called ACF (amplifier correction factor). The ACF represents the mean correction in dB, which is needed to get a flat power response.

Compared to other approaches this simulation model is based on a certain frequency range and not by the number of modes [9]. A frequency range from 100 Hz to 1000 Hz was chosen because it represents a range with high deviation as a result of lower modal density. This paper presents a simulation model for computing the radiated sound power of different sized panels with varying aspect ratios, excited by a two-dimensional driver array of 100 drivers applied to the panel. The model is based on the commercial FEA and BEM software tool wave6 [10].

A short summary of the plate mechanics, which describe the most important relationships of material properties, is presented. This chapter emphasizes the limitations of current methods. Furthermore, the ACF is introduced, and the whole workflow of the simulation is presented. Three different sized panels are compared in order to demonstrate various designs as well as improvements, which cannot be identified with traditional design methods.

This approach will help loudspeaker designers to get a better understanding of the influence of exciter placement depending on the surface area and aspect ratio of the panel.

2 Modal behavior of plates

This section is a summary of plate mechanics and its relevance for this paper. A more detailed description can be found in Fahy and Gardonio [11].

2.1 Modal behavior of plates

There are several approaches to describe the vibration behavior of plates. The most important plate mechanics for this simulation model are presented below. It is important to differentiate modal density and lowest natural frequency. The modal density is the number of modes per frequency, and the lowest natural frequency is the frequency value of the mode with indices (1, 1).

An empirical formula for the modal density is given by Fahy and Gardonio [11]

$$n(f) = \left(\frac{A}{2}\right)\left(\frac{\rho_A}{D}\right)^{\frac{1}{4}} \tag{1}$$

where D is the 'bending stiffness' and ρ_A 'density per unit area' of the plate. The modal density depends on the area A and material parameters. The modal density is defined as the number of modes per frequency band with a linear frequency spacing. Compared to the human perception of a logarithmic frequency spacing, it will result in a lack of modes at low frequencies and a high modal overlap at high frequencies.

The aspect ratio does not affect the modal density and affects the lowest natural frequency. The aspect ratio R is defined by the plate dimensions L_x and L_y

$$R = \frac{L_x}{L_y}. \tag{2}$$

Mitchell and Hazell [12] provided an equation to describe the natural frequency ω of a plate with fully clamped edges for each mode, characterized by mode indices m and n. This approach is also used by Anderson to describe a DML simulation model [13] with

$$\omega^2 = \left[\frac{\pi^4 D}{\rho_A}\right]\left[\left(\frac{m+\Delta_m}{L_x}\right)^2 + \left(\frac{n+\Delta_n}{L_y}\right)^2\right]^2 \tag{3}$$

where

$$\Delta m = \frac{1}{\left(\frac{nL_x}{mL_y}\right)^2 + 2} \quad and \quad \Delta n = \frac{1}{\left(\frac{mL_y}{nL_x}\right)^2 + 2} \tag{4}$$

An overview of all natural frequencies up to 400 Hz for three different surface areas is shown in Fig. 1. It indirectly presents the lowest natural frequency and the modal density. This modal analysis is performed with the FE-solver of the software tool wave6. Larger surface areas will result in a lower natural frequency and higher modal density.

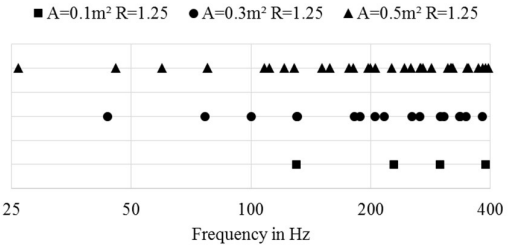

Fig. 1: All natural frequencies until 400Hz for three different surface areas with an aspect ratio of 1.25.

2.2 Modal overlap and its influence for the positioning

The behavior of DML is based on a set of modes. Driven by a point force, a combination of these modal shapes are excited and can be written as a superposition of individual modes shown in Fig. 2. If there are modes with a large frequency spacing, then the response is dominated by individual modes or distinct resonances.

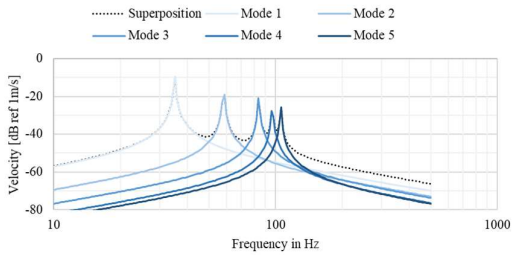

Fig. 2: Magnitude of velocity transfer function of the first five modes simulated as single modes and as a superposition of all modes.

As frequency spacing between modes decreases and damping increases, it becomes more difficult to identify modes which dominate the response. This is the result of a modal overlay, which is demonstrated in Fig. 3. For high damping values, no distinct resonances for mode 3 to mode 5 can be identified.
It is conceivable to describe a frequency, where the response is no longer dominated by distinct resonances, and it is not important to drive every single mode.

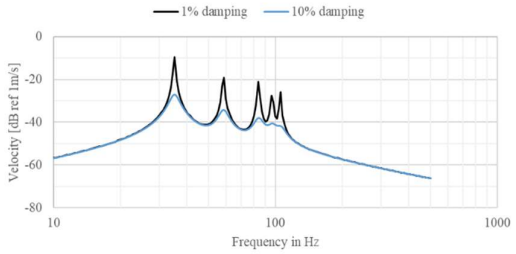

Fig. 3: Magnitude of velocity transfer function with 1% damping compared to 10% damping. Higher damping values enhance the modal overlap, and distinct modes are not visible.

2.3 Point force driver locations based on State of the Art methods

The DML technology represents an interference and destructive interference between incident waves and reflected waves. The results are standing wave patterns that produce locations with strong out-of-plane motion and locations with no out-of-plane motion. The nodes are locations with no out-of-plane motion and represent a high impedance. Therefore, they are not suitable as excitation location for a transducer. In a two-dimensional system, the node points collectively form nodal lines. Good exciter positions were defined by Bank as drive points [6]. These are exciter locations, which are not located on any nodal lines. It is still State of the Art to analyze the panel for nodal lines [14].
To visualize this idea with modern FE-Software a superposition of individual modes is presented. All modes are normalized, based on their maximum displacement x_{max} to a maximum value of 1 and a minimum value of 0. The normalized displacement is defined with x_{Norm}. Furthermore, all values are calculated as an absolute value to avoid the phase influence of every mode shape. To emphasize regions with less displacement, the value of x_{Norm} is calculated with the potential of 0.3.

$$x_{Norm}(n_{Mode}, L_{x,y}) = \left(\frac{|x_{Modal}(n_{Mode}, L_{x,y})|}{|x_{max}|}\right)^{0.3} \quad (5)$$

Fig. 4 represents the normalization process of mode number 50 and the weighting of nodal lines. To visualize nodal lines, the following Fig. 5 shows a superposition of the first nine modes of a plate with fixed boundary conditions and a ratio of R = 1.25.

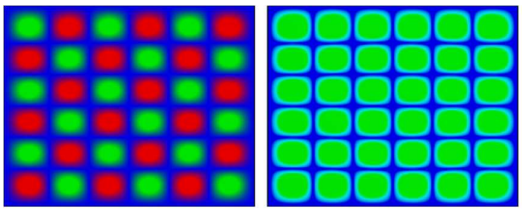

Fig. 4: Comparison of normal mode displacement and the absolute value plot with nodal weighting for mode number 50 of the FE-solver.

The advantage of taking the full FE model, compared to the nodal lines, becomes evident by taking a closer look at the center lines and the border. These center lines and borders are areas with nearly no out-of-plane motion.

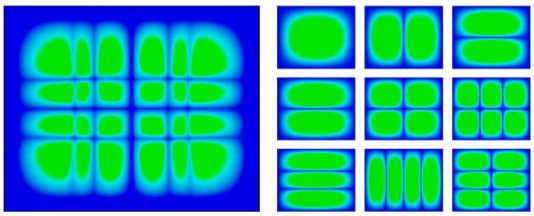

Fig. 5: Superposition of nine mode shapes of a plate with fixed boundary conditions to visualize the nodal lines and areas of a possible good excitation.

For a panel with fixed boundary conditions, the strongest displacement is located around the center and decreases to zero at the edges. At the center lines, it is a result of the symmetric shape of nearly all modes, due to the fixed boundary conditions.
In [6] it is recommended to initially consider the first 20 modes, in order to find suitable drive point locations. A number of possible drive point locations are presented in Table 1.

Name of location	L_x	L_y
Exciter 1	45 %	40 %
Exciter 2	15 %	20 %

Table 1. Chosen points for following comparison of optimal drive points.

To visualize the idea of superpositioning, the following Fig. 6 shows the superposition of the first 20 modes.
It is shown that good candidates are out of the center lines and at least 15 % away from the edges. As a result of simulating homogeneous materials with symmetric shape, all modes are symmetric with respect to the central location [50 %, 50 %]. A homogeneous material has the same material and thickness properties in the entire subsystem. For this reason, it is sufficient to focus on one-quarter of the panel in the following steps.

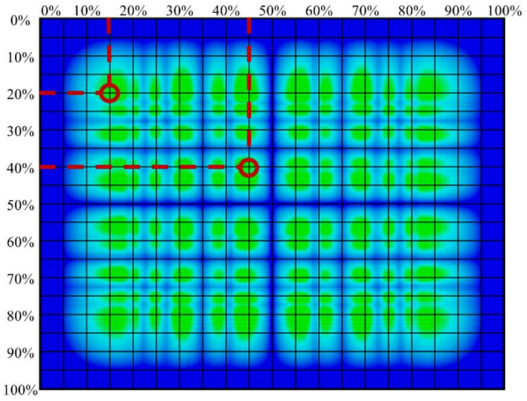

Fig. 6: Superposition of the first 20 modes of a plate with an aspect ratio of 1.25. Chosen Exciter 1 and Exciter 2 are marked for further comparisons.

3 Simulations

This part introduces the concept of the simulation model and its evaluation based on a singular criterion named ACF (amplifier correction factor).

3.1 Simulation properties

The simulation is based on an acrylic panel with a thickness of 3 mm. The material properties were determined with modal analysis by a model fitting from measurements and FE simulations and applied to every model.
The resulting properties are $D = 22.6\,Nm$ and $\rho_A = 4.74\,kg/m^2$. An experimentally measured damping loss factor of 3 % is additionally applied to the panel and 1 % as damping loss factor in the BEM subsystem. All modes are calculated up to 1100 Hz to get their influence on the frequency response. The model employs the finite element method (FEM) to represent the structural domain, and the boundary element method (BEM) to represent the acoustic domain. Full coupling between the structural and acoustic domains is taken into account. The mesh size for the FEM-subsystem is based on six elements per bending wavelength meshed with CQUAD8 mesh. The worst case is a small surface area with high aspect ratio. For such cases, the number of elements is locally increased, such that there is a separate node for each excitation location.

The exciter force is calculated based on an electromechanical model shown in Fig. 7. The chosen exciter is the Visaton EX60S.

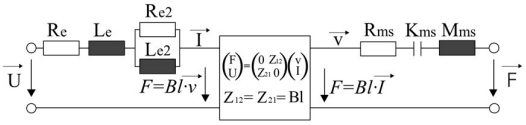

Fig. 7: An electromechanical model of an exciter with a fixed magnet.

All parameters of the electromechanical model have been measured with the Klippel distortion analyzer and are listed in Table 2.

Parameter	Values	Description of parameters
fs,mag	58.3 Hz	Magnet resonance frequency
Re	7.54 Ohm	Electrical VC resistance at DC
Le	0.141 mH	Frequency independent part of the VC
Re2	0.94 Ohm	Electrical resistance due to eddy current losses
Le2	0.226 mH	Para-inductance of voice coil
Bl	5.016 N/A	Force factor
Kms	15.54 N/mm	Mechanical stiffness of driver suspension
Rms	5.648 kg/s	Mechanical resistance of total-driver losses
Mms,plate	14.112 g	Mechanical mass of Plate

Table 2. Measured electromechanical parameters of Visaton EX60S

The exciter is driven by a voltage amplitude of 1V. In contrast to a full two-dimensional vibration system, the point force represents a single degree of freedom. It can't represent the full exciter, because of the missing degree of freedom for the moving mass. Therefore, this model corresponds to an exciter with a clamped magnet. The risk of failure is low, because of the low resonance frequency compared to the considered frequency range.

3.2 Definition of a singular evaluation criterion

It is required to reduce the power transfer functions to a single value to consider all power transfer functions. This quality index is called ACF (amplifier correction factor). This value represents a mean correction in dB, which is required to get a flat power transfer response.

These corrections can be done, e.g., with a DSP amplifier. As the ACF becomes smaller, less correction is needed to get a flat power transfer response. It represents the flatness of the power transfer function. One might think that this value is just the standard deviation of its power transfer function, but the ACF references the average maximum power value of each surface area with a certain aspect ratio. It rates exciter positions with less average power values worse, compared to positions with higher power values. This maximum power value $L_{W,Max}$ is calculated with the following equation:

$$L_{W,Max} = max\left(\frac{1}{n_f}\sum_{f=f_l}^{f_h} L_{W,f}(P)\right) \tag{6}$$

$L_{W,Max}$ represents the maximum power value of all positions P for a certain area A with a certain aspect ratio R. The calculation of ACF is based on the standard deviation of every single power transfer function to a flat response of $L_{W,max}$ [15]. The standard deviation gives the advantage to evaluate stronger dips and peaks higher in comparison to smaller deviations.

$$ACF = \sqrt{\frac{1}{n_f - 1}\sum_{f=f_l}^{f_h}\left(L_{W,f} - L_{W,Max}\right)^2} \tag{7}$$

ACF is calculated in the frequency range between the lowest frequency f_l and the highest frequency f_h, and is defined in dB. A value of 0 dB represents an ideal flat sound power response. A power transfer function is shown in Fig. 8, which has an ACF of 2.7 dB.

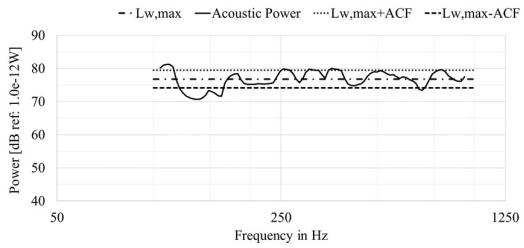

Fig. 8: Radiated sound power presented with the calculated ACF values of a single exciter on a plate.

3.3 Workflow of the Simulation

The full simulation model is scripted with python in wave6. Fig. 9 shows the whole workflow up to the ACF calculation.

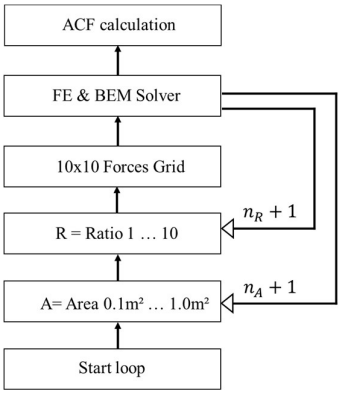

Fig. 9: Workflow of the simulation model.

The simulation is performed for ten different surface areas and ten different aspect ratios. A list of all areas and ratio can be found in Table 3.

Name	Values
Area A, m²	0.1, 0.2, 0.3, 0.4, 0.5, 0.6, 0.7, 0.8, 0.9, 1.0
Ratio R	1.0, 1.25, 1.5, 2.0, 2.5, 3.0, 3.5, 4.0, 5.0, 10.0

Table 3. List of areas and ratios simulated in this model.

The plate is driven with an exciter, abstracted as point force. The forces are automatically placed on a 10x10 grid in the 2nd square of the DML panel shown in Fig. 10. With these steps a subdivision of 5 % is possible, and the placement on the symmetric lines are included.

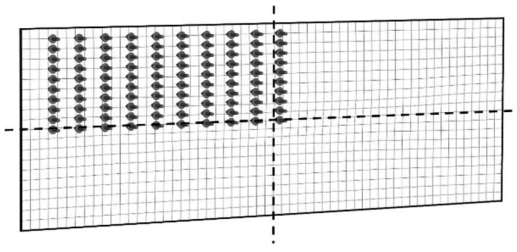

Fig. 10: Simulation model with a 2D grid of 100 point forces and the marked center lines.

In order to reduce the simulation time, all exciters are placed in one quadrant, because of:

- The symmetrical shape of the plate,
- Symmetrical boundary conditions,
- Force of one exciter and
- Homogeneous material.

In contrast to Anderson [9] the simulation is based on a frequency range and not on the number of modes. The chosen frequency range is from 100 Hz to 1000 Hz. The frequency range is arbitrarily expandable to lower or higher frequencies but represents the part of the transfer function with most deviations, a consequence of the modal density.

4 Results

This chapter presents three examples to compare the chosen drive-points with the best available positions for different surface areas. Furthermore, the best positions of aspect ratio 1.25 are compared with the best values of all aspect ratios.

4.1 Detailed evaluation

All simulations are based on the acrylic panel. The following areas are chosen to visualize the influence of the surface area on the drive point location:

- Example 1 has a surface area of 0.1 m², which results in less modal density and distinct modes in the frequency range,
- Example 2 has a surface area of 0.5 m² and results in a 5 x higher modal density and larger modal overlap,
- Example 3 has a surface area of 1.0 m² and results in a 2 x higher modal density compared to 0.5 m².

The simulated ACF values for the chosen surface areas and the selected transfer functions are shown in Fig. 11 - Fig. 13. The ACF enables the comparison of different surface areas and aspect ratios. There is no single position, which is the best position for all areas. For a smaller surface, the panel is divided into good and bad excitation areas showing in Fig. 11.

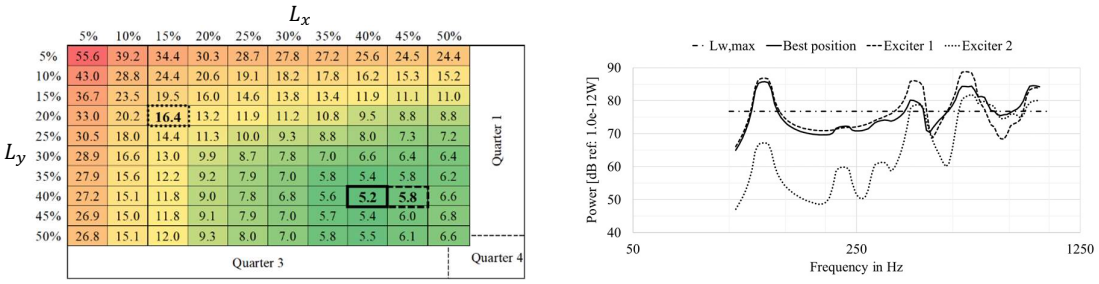

Fig. 11: (a) ACF values for the area of 0.1 m² with an aspect ratio of 1.25. The chosen positions for Exciter 1, Exciter 2 and the best position are marked. These marked values are representing transfer functions, which are plotted in (b). The transfer function of the radiated sound power is plotted for the two chosen Exciter positions and the best available position (L_x=40%, L_y=40%).

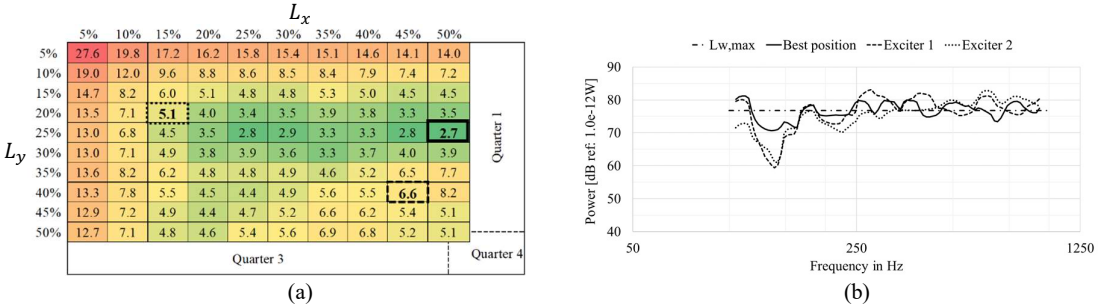

Fig. 12: (a) ACF values for the area of 0.5 m² with an aspect ratio of 1.25. The chosen positions for Exciter 1, Exciter 2 and the best position are marked. These marked values are representing transfer functions, which are plotted in (b). The transfer function of the radiated sound power is plotted for the two chosen positions and the best available position (L_x=50%, L_y=25%).

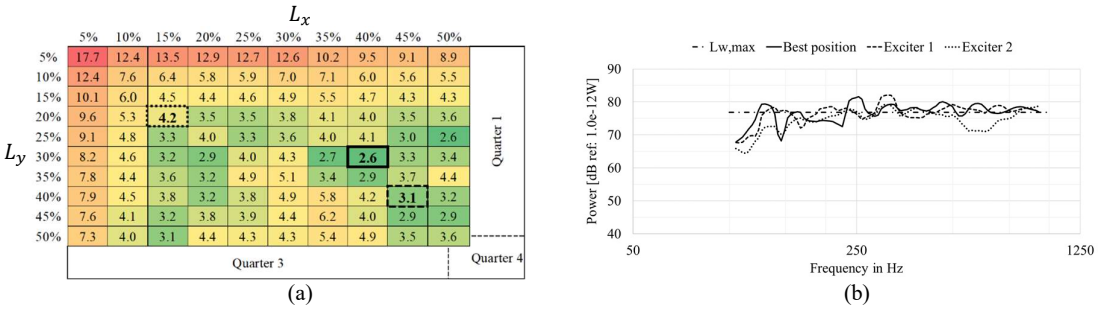

Fig. 13: (a) ACF values for the area of 1.0 m² with an aspect ratio of 1.25. The chosen positions for Exciter 1, Exciter 2 and the best position are marked. These marked values are representing transfer functions, which are plotted in (b). The transfer function of the radiated sound power is plotted for the two chosen positions and the best available position (L_x=40%, L_y=30%).

The lowest ACF value of 5.2 dB represents a high deviation, and a DSP correction is recommended. The best exciter positions are close to the results of Exciter 1, calculated with the nodal lines. In general, the exciter should not be placed in the center. 10 % off center for both axes is nearly perfect. Furthermore, it is important to keep a certain distance to the border. The location of Exciter 2 is too close to the border, and it is not possible to get enough energy into the panel. A high average DSP correction of 16.4 dB is needed.

The results for larger surface areas are shown in Fig. 12 and Fig. 13. Increasing the area results in smaller average ACF values. The best ACF values are nearly equal for surface area 0.5 m² and 1.0 m². Surface area 1.0 m² has more positions with lower ACF values, but they are arbitrarily located. The best positions cannot be identified by the modes due to the large modal overlap. In conclusion, it is not important to excite every single mode to get a flat sound power response.

4.2 General evaluation

In addition to the results of 4.1, it is possible to search for the best ACF values. Fig. 14 shows the area dependent best ACF values for an aspect ratio of 1.25. For small areas (< 0.3 m²) the best achievable values are close to Exciter 1, based on nodal lines. For larger surface areas (> 0.3 m²) the potential of a detailed simulation is presented by the difference of the ACF values for Exciter 1,2 and the best position. Improvements of ca. 2 dB are possible to achieve deviations of less than 3 dB.

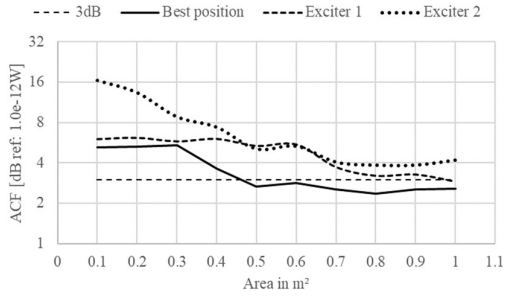

Fig. 14: Area dependent ACF values for an aspect ratio of 1.25. Values for Exciter 1 and Exciter 2 are compared to the best ACF values.

The best positions cannot be identified by a superposition of the first modes due to the large modal overlap. Despite precise positioning it is recommended to use a DSP for small areas (< 0.3 m²), to get closer to the flatness of a cone loudspeaker.

5 Conclusions

The exciter placement is one of the most important parts of the design process of panel loudspeakers. This paper has shown another idea to find the best position by optimizing the radiated sound power response. The acrylic panel DML is simulated for nearly all possibilities of surface areas, aspect ratios and driver positions. Instead of the traditional design method by a superposition of the first eigenmodes a full acoustic simulation model, based on the FEM and BEM methods, was used for the analysis. The whole simulation workflow is scripted in wave6 and extendable to more complex topics like the following:

- Second exciter or even more,
- Wider frequency range and
- Different materials (anisotropic).

The authors introduce a single comparison value named ACF, which represents the deviation of the radiated sound power response. The ACF has been confirmed as a suitable criterion to differentiate all transfer functions based on a single value. This allows a comparison of the best design parameters for different surface areas and aspect ratios.

For small areas with distinct modes, it is easier to find the best positions. These best positions have still 5dB deviation, and a DSP filtering of the input signal is recommended.

For larger surface areas the average ACF decreases. Values until 2.7 dB are possible. These positions are more arbitrarily located, and simulation software is needed to find these best positions. Potentials of 3 dB are possible compared to standard positions.

This paper investigates the influence of the exciter location on the acoustic performance of a DML, and it helps to get a better understanding of DML speaker design. Furthermore, this idea will find the best positions for a flat radiated sound power response to realize significant improvements of the acoustic performance compared to designs using traditional design methods.

6 Acknowledgments

The authors are grateful to ZIM (project number ZF4444801) for the support of this study. They also thank the Hommbru Company and wave6 as partners of this project.
The results of this study representing the research work of the cooperation of Hommbru and the University of Technology Dresden.

References

[1] J. Panzer and N. Harris, "Distributed-Mode Loudspeaker Radiation Simulation," presented at the *105th convention of the Audio Engineering Society* (1998), convention paper 8397.

[2] H. Azima, J. Panzer, and D. Reynaga, "Distributed-Mode Loudspeakers (DML) in Small Enclosures," presented at the *106th convention of the Audio Engineering Society* (1999), convention paper 8193.

[3] G. Bank and N. Harris, "The Distributed Mode Loudspeaker-Theory and Practice," presented at the *Audio Engineering Society Conference: UK 13th Conference: Microphones & Loudspeakers* (1998).

[4] Basilio Pueo, Jose Escolano-Carrasco, Jose Javier Lopez, and German Ramos, "A Note on the Filtering Equalization in Large Multiactuator Panels," presented at the *17th European Signal Processing Conference (EUSIPCO 2009)* (2009).

[5] M. M. Boone, "Multi-Actuator Panels (MAPs) as Loudspeaker Arrays for Wave Field Synthesis," (English), *JAES*, vol. 52, no. 7/8, pp. 712–723 (2004).

[6] G. Bank "The distributed mode loudspeaker (DML)" in J. Borwick, *Loudspeaker and headphone handbook,* 3rd ed. Oxford: Focal Press, 2001.

[7] D. A. Anderson, M. C. Heilemann, and M. F. Bocko, "Optimized Driver Placement for Array-Driven Flat-Panel Loudspeakers," *Archives of Acoustics*, vol. 42, no. 1, pp. 93–104 (2017).

[8] L. Hörchens and D. de Vries, "Comparison of Measurement Methods for the Equalization of Loudspeaker Panels Based on Bending Wave Radiation," presented at the *130th convention of the Audio Engineering Society* (2011), convention paper 15792.

[9] D. A. Anderson, M. C. Heilemann, and M. F. Bocko, "Flat-Panel Loudspeaker Simulation Model with Electromagnetic Inertial Exciters and Enclosures," (English), *JAES*, vol. 65, no. 9, pp. 722–732 (2017).

[10] wave6, "version 2018.10.4," *Dassault Systemes SIMULIA Corp*, available at www.wavesix.com.

[11] F. Fahy and P. Gardonio, *Sound and structural vibration,* 2nd ed. Amsterdam, London: Elsevier/Academic, 2007.

[12] A. K. Mitchell and C. R. Hazell, "A simple frequency formula for clamped rectangular plates," *Journal of Sound and Vibration*, vol. 118, no. 2, pp. 271–281 (1987).

[13] D. Anderson, M. Heilemann, and M. F. Bocko, "Impulse and Radiation Field Measurements for Single Exciter versus Exciter Array Flat-Panel Loudspeakers," presented at the *143rd convention of the Audio Engineering Society* (2017 Oct), convention paper 19330.

[14] Timothy Christopher Whitwell, "Audio Transducer Stabilization System and Method," US20160219353A1, U.S. Patent 14/604,580, Aug. 26, 2015.

[15] S. Birkedal Nielsen and A. Celestinos, "Optimizing Placement and Equalization of Multiple Low Frequency Loudspeakers in Rooms," presented at the *119th convention of the Audio Engineering Society* (2005), convention paper 13307.